arXiv:0809.3583v2 [quant-ph] 4 Mar 2010

Teleportation-Based Controlled-NOT Gate for Fault-Tolerant Quantum Computation

Alexander M. Goebel[1], Claudia Wagenknecht[1], Qiang Zhang[2], Yu-Ao Chen[1,2], and Jian-Wei Pan[1,2]
[1] *Physikalisches Institut, Ruprecht-Karls-Universität Heidelberg, Philosophenweg 12, 69120 Heidelberg, Germany*
[2] *Hefei National Laboratory for Physical Sciences at Microscale and Department of Modern Physics, University of Science and Technology of China, Hefei, Anhui 230026, China*

(Dated: March 4, 2010)

Quantum computers promise dramatic speed ups for many computational tasks. For large-scale quantum computation however, the inevitable coupling of physical qubits to the noisy environment imposes a major challenge for a real-life implementation. A scheme introduced by Gottesmann and Chuang can help to overcome this difficulty by performing universal quantum gates in a fault-tolerant manner. Here, we report a non-trivial demonstration of this architecture by performing a teleportation-based two-qubit controlled-NOT gate through linear optics with a high-fidelity six-photon interferometer. The obtained results clearly prove the involved working principles and the entangling capability of the gate. Our experiment represents an important step towards the feasibility of realistic quantum computers and could trigger many further applications in linear optics quantum information processing.

PACS numbers: 03.65.Ud, 03.67.Mn, 42.50.Dv, 42.50.Xa

In theory, quantum computers can outperform their classical counterparts in various computational tasks such as searching an unsorted data base [1] or factorizing large numbers [2]. They further promise efficient simulation of dynamics of complex quantum systems, which is not possible with conventional computers [3]. Practical implementations, however suffer severely from coupling to the noisy environment and residual imperfections in physical systems [4–6].

Any system in nature couples to its environment. In quantum computation this can lead to errors among the processed qubits making quantum error correction schemes necessary. Several algorithms to encode a logic qubit onto a number of physical qubits have been developed [7–12]. These codes are able to correct for any single qubit error, as long as maximally one of the physical qubits has been altered. After decryption one is able to recover the unaltered, original logic qubit. A next problem arises once we want to perform quantum gates, i.e. to perform logic operations on the protected data. Since the logic qubit has been encoded, we need to perform corresponding operations on the physical qubits. Depending on the characteristics of the chosen code and gate (in particular conditional gates), errors may then not only propagate between blocks of encoded qubits but also within them. This can compromise the code's ability to correct for these errors. The solution are the so-called "fault-tolerant quantum gates". A procedure is fault-tolerant if its failing components (including the the errors in the encoded input qubits) do not spread more errors in the block of encoded output qubits than the code can correct.

In a seminal paper, Gottesman and Chuang introduced a novel protocol to implement any quantum gate needed for quantum computation in a fault-tolerant manner [13]. Their work has opened doors to new ideas and has triggered several important protocols in theoretical quantum information processing, such as one-way quantum computation [14] and linear optics quantum computation [15]. Although there is fast progress in the theoretical description of quantum information processing, the difficulties in handling quantum systems have not allowed an equal advance in the experimental realization of the new proposals. Up to now, not even a proof-in-principle demonstration of a teleportation-based quantum logic gate, the fundamental building block of the Gottesman-Chuang (GC) scheme, has been realized.

In this Letter, we report a non-trivial realization of the GC scheme. We develop and exploit a high-fidelity six-photon interferometer to combine the techniques of quantum teleportation of a composite system [16] and the creation of a four-qubit photon cluster state [17]. In the experiment, we chose to implement a teleportation-based controlled-NOT (C-NOT) gate, which, together with very easy to implement single qubit operations, is sufficient to perform all logic operations needed for quantum computation [18, 19]. Compare to the previous six-photon experiments [16, 20] our experimental setup is more complex and involves more interferences. Various efforts have been made to achieve the stringent fidelity requirements and sufficient six-photon count rate.

The approach of Gottesman and Chuang, a generalization of quantum teleportation [21, 22], is straight forward and requires only a minimum of resources. A key element of their work is the C-NOT gate, which acts on two qubits, a control and a target qubit. The logic table of the C-NOT operation (U^{C-NOT}) is given by $|H\rangle_1|H\rangle_2 \rightarrow |H\rangle_1|H\rangle_2$, $|H\rangle_1|V\rangle_2 \rightarrow |V\rangle_1|V\rangle_2$, $|V\rangle_1|H\rangle_2 \rightarrow |V\rangle_1|H\rangle_2$ and $|V\rangle_1|V\rangle_2 \rightarrow |H\rangle_1|V\rangle_2$, where we have used the photon polarization degree of freedom to encode our qubits. A schematic diagram of the procedure can be observed in Fig. 1A. One starts with the two input qubits $|T\rangle_1$ (target) and $|C\rangle_2$ (control). Instead of directly performing complicated gate operations on the input qubits, one prepares in forehand a special entangled four-qubit state

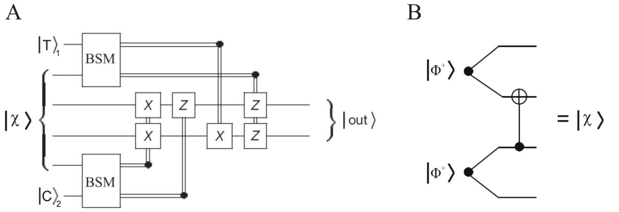

FIG. 1: Quantum circuit for teleporting two qubits through a C-NOT gate. Time flow is from left to right. The input consisting of the target qubit $|T\rangle_1$ and control qubit $|C\rangle_2$ can be arbitrarily chosen. Bell State Measurements (BSMs) are performed between the input states and the outer qubits of the special entangled state $|\chi\rangle$. Depending on the outcome of the BSMs, local unitary operations (X, Z) are conducted on the remaining qubits of $|\chi\rangle$, which then form the output $|out\rangle = U^{C-NOT}|T\rangle_1|C\rangle_2$. Single lines correspond to qubits and double lines represent classical bits. **(B)** The special entangle state $|\chi\rangle$ can be constructed by performing a C-NOT gate on two EPR pairs, with $|\Phi^+\rangle = \frac{1}{\sqrt{2}}(|H\rangle|H\rangle + |V\rangle|V\rangle)$.

$|\chi\rangle$. After verification that the creation of $|\chi\rangle$ was successful, one transfers the data of the input qubits onto $|\chi\rangle$ by quantum teleportation. This is done by successively performing a joint "Bell-State-Measurement" (BSM) between the target (control) qubit and an outer qubit of $|\chi\rangle$, i.e. one projects the target (control) qubit and one of the outer qubits of $|\chi\rangle$ onto a joint two-particle "Bell state". As a direct consequence of the projective BSMs and the four-partite entanglement of $|\chi\rangle$, the remaining two (output) qubits already posses the information originally carried by the input qubits, i.e. the input state is teleported onto the four-particle state $|\chi\rangle$. To finish the procedure – just like in the original teleportation scheme – we need to apply single qubit (Pauli) operations to the output qubits, depending on the outcome of the BSMs.

Due to the special entanglement characteristics of $|\chi\rangle$, the output state is equivalent to the desired unitary transformation of the input state given by

$$|out\rangle = U^{C-NOT}|T\rangle_1|C\rangle_2. \tag{1}$$

This can be better understood by a closer look at the special entangled state $|\chi\rangle$. It is a four-particle cluster state [23] of the form

$$\begin{aligned}|\chi\rangle = \frac{1}{2}((|H\rangle|H\rangle + |V\rangle|V\rangle)|H\rangle|H\rangle \\ +(|H\rangle|V\rangle + |V\rangle|H\rangle)|V\rangle|V\rangle).\end{aligned} \tag{2}$$

which can be created simply by performing a C-NOT operation on two EPR pairs as can be seen in Fig. 1B. This C-NOT operation is the essential difference to the original teleportation scheme and is the reason for the fact that the output state is not identical to the input state, but rather in the desired form of Eq. 1. A detailed discussion of the scheme is given in the supplementary information.

Note, that in the above scheme all qubits are logic qubits. However, the scheme generalizes in a straight forward manner when we use a larger number of physical qubits to encode our logic qubits. The procedure is then fault-tolerant since all operations are transversal, i.e. qubits of one block of encoded qubits interact only with corresponding qubits in other code blocks. A further advantage is the fact that only classically controlled single-qubit operations and BSMs are needed to perform the actual gate. The resource of the special entangled state $|\chi\rangle$ can be constructed in forehand. If its generation fails nothing is lost by discarding it and trying again until successful generation. We would like to emphasize two aspects: First, the setup can be used to process any unknown input state and second, several other quantum gates can be implemented by this scheme. The choice of gate only depends on the form of the ancillary state $|\chi\rangle$.

A schematic diagram of our experimental setup is shown in Fig. 2. All three photon pairs are originally prepared in the Bell-state $|\Phi^+\rangle = \frac{1}{\sqrt{2}}(|H\rangle|H\rangle + |V\rangle|V\rangle)$. We observe on average 7×10^4 photon pairs per second from each (EPR) source. With this high-intensity entangled photon source we obtain in total 3.5 six-photon events per minute. This is less than half the count rate of our previous six-photon experiments [16, 20, 25]. Since the new scheme is more complex and involves more interferences, the fidelity requirements are more stringent. Thus, we have to reduce the pump power from 1.0 W to 0.8 W in order to reduce noise contributions that arise from the emission of two pairs of down-converted photons by a single source (double-pair-emission).

With the help of wave plates and polarizers, we prepare photon pair 1&2 in the desired two-qubit input state $|\Psi\rangle_{12}$. Photon pairs 3&4 and 5&6, which are both in the state $|\Phi^+\rangle$, are used as a resource to construct the special entangled state $|\chi\rangle_{3456}$.

Among the existing various methods for preparing the four-photon cluster state $|\chi\rangle_{3456}$, however, only [17] works in our present experiment as others are vulnerable to double-pair-emission. As shown in Fig. 2 photons 4 and 6 are interfered on a beam splitter with a polarization-dependent splitting ratio (PDBS), i.e. the transmission for horizontal (vertical) polarization is $T_H = 1$ ($T_V = 1/3$). In order to balance the transmission for all input polarizations, beam splitters (PDBS') with reversed transmission conditions ($T_H = 1/3$, $T_V = 1$) are placed in each output of the overlapping PDBS. Altogether, the probability of having one photon in each desired output, and thus having successfully created the cluster state, is 1/9. Half wave plates (HWPs) in arms 3 and 4 are used to transform the cluster state to the desired state by local unitary operations.

With our high power EPR-source we are able to

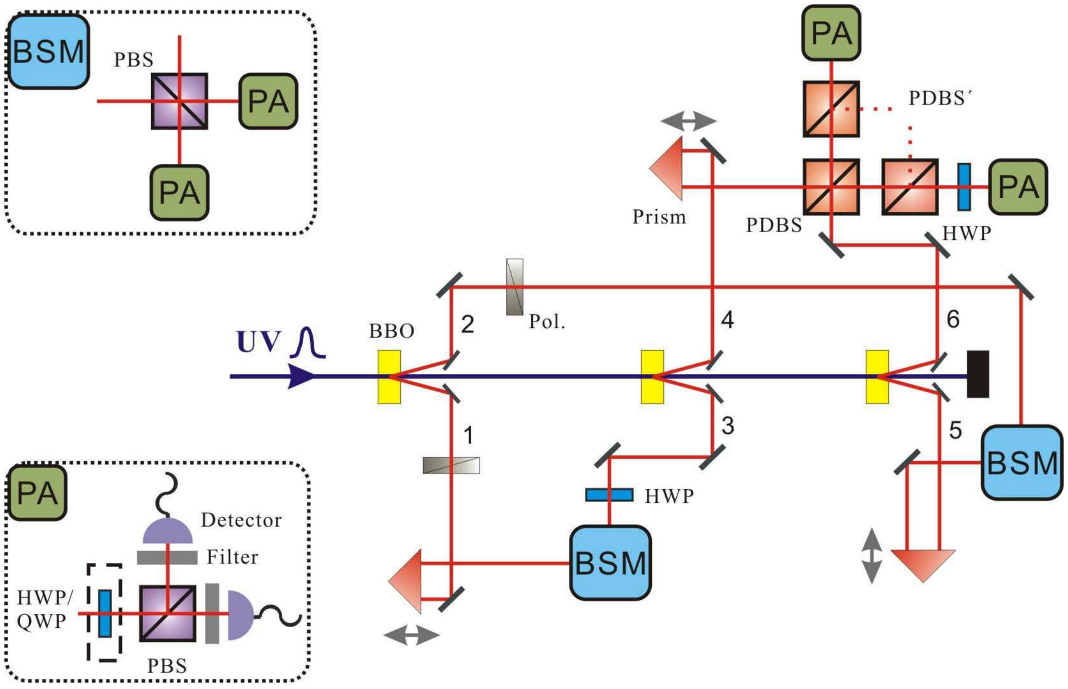

FIG. 2: A schematic diagram of the experimental setup. A high-intensity pulsed ultraviolet laser beam (UV) at a central wavelength of 390 nm, a pulse duration of 180 fs, and a repetition rate of 76 MHz successively passes through three β-barium borate (BBO) crystals to generate three polarization entangled photon pairs via type-II spontaneous parametric down-conversion [24]. At the first BBO the UV generates a photon pair in modes 1 and 2 (i.e. the input consisting of the target and control qubit). After the crystal, the UV is refocused onto the second BBO to produce another entangled photon pair in modes 3 and 4 and correspondingly for modes 5 and 6. Photons 4 and 6 are then overlapped at a PDBS and together with photons 3 and 5 constitute the cluster state. Two PDBS' are used for state normalization. The prisms are mounted on step motors and are used to compensate the time delay for the interference at the PDBS and the BSMs. A BSM is performed by overlapping two incoming photons on a PBS and two subsequent polarization analyses (PA). A PA projects the photon onto an unambiguous polarization depending on the basis determined by the choice of half or quarter wave plate (HWP or QWP). The photons are detected by silicon avalanched single-photon detectors. Coincidences are recorded with a coincidence unit clocked by the infrared laser pulses. Pol. are polarizers to prepare the input state and Filter label the narrow band filters with $\Delta_{FWHM} = 3.2$ nm.

achieve a count rate for the four-qubit cluster state $|\chi\rangle_{3456}$ that is two orders of magnitude larger than in a recent experiment [17]. We have measured the fidelity of $|\chi\rangle_{3456}$ and obtain an experimental result of 0.694 ± 0.003, which is only slightly lower than in [17] due to the much higher pump power. The fidelity measurement has been performed in complete analogy to Kiesel et al. [17]. The improvement of the count rate is necessary in order to be able to perform the six-photon experiment in a reasonable amount of time over which the experimental setup can be kept stable.

Teleporting the input data of $|\psi\rangle_{12}$ to $|\chi\rangle_{3456}$ requires joint BSMs on photons 1&3 and photons 2&5. To demonstrate the working principle of the teleportation-based C-NOT gate, it is sufficient to identify one of the four Bell states in both BSMs [16, 20]. However, in the experiment we decide to analyse the two Bell states $|\Phi^+\rangle$ and $|\Phi^-\rangle$ to increase the efficiency - the fraction of success - by a factor of 4. This is achieved by interfering photons 1&3 and photons 2&5 on a polarizing beam splitter (PBS) and performing a polarization analysis (PA) on the two outputs[26]. With the help of a HWP, a PBS and fibre-coupled single photon detectors, we are able to project the input photons of the BSM onto $|\Phi^+\rangle$ upon the detection of a $|+\rangle|+\rangle$ or $|-\rangle|-\rangle$ coincidence, and onto $|\Phi^-\rangle$ upon the detection of a $|+\rangle|-\rangle$ or $|-\rangle|+\rangle$ coincidence (where $|\pm\rangle = (|H\rangle \pm |V\rangle)/\sqrt{2}$). The increasing of success efficiency allow us reducing the pump power in order to reduce noise contributions while preserving the overall count rate.

The projective BSMs between the data input photon 1 (2) and photon 3 (5) of the cluster state leave the remaining photons of the cluster state 4&6 up to a unitary transformation in the state $|out\rangle_{46}$. This is the desired final state of having performed a C-NOT operation on photons 1&2. To demonstrate that our teleportation-based C-NOT gate protocol works for a general unknown polarization state of photons 1&2, we decide to measure

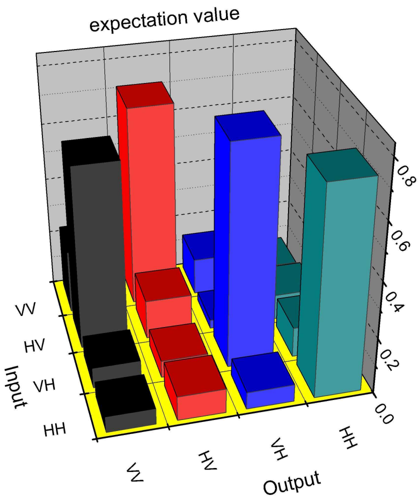

FIG. 3: Experimental results for truth table of the C-NOT gate. The first qubit is the target and the second is the control qubit. The average fidelity for the truth table is 0.72 ± 0.05.

the truth table of our gate. That is, we measure the output for all possible combinations of the two-qubit input in the computational basis. However, that is not sufficient to show the quantum characteristic of a C-NOT gate. The remarkable feature of a C-NOT gate is its capability of entangling two separable qubits. Thus, to fully demonstrate the successful operation of our protocol, we furthermore choose to perform the entangling operation:

$$|H\rangle_T \otimes \tfrac{1}{\sqrt{2}}(|H\rangle_C + |V\rangle_C) \xrightarrow{C-NOT}$$
$$\tfrac{1}{\sqrt{2}}(|H\rangle_T|H\rangle_C + |V\rangle_C|V\rangle_C) = |\Phi^+\rangle_{TC} \qquad (3)$$

We quantify the quality of our output state by looking at the fidelity as defined by $F = Tr(\hat{\rho}|out\rangle\langle out|)$ where $|out\rangle$ is the theoretically desired final state and $\hat{\rho}$ is the density matrix of the experimental output state. To analyze the operation and to experimentally measure the fidelity of the two-qubit output, we again use PAs. Depending on the measurement setting we use quarter wave plates (QWP) or HWP in front of the PBS.

The fidelity measurements for the truth table are straightforward. Conditional on detecting a fourfold coincidence at the two BSMs, we analyze the output photons 4&6 in the computational H/V basis. Depending on the type of coincidence at the BSM ($|+\rangle|+\rangle$, $|+\rangle|-\rangle$, $|-\rangle|+\rangle$, $|-\rangle|-\rangle$), i.e. depending onto which Bell state the photons have been projected, we analyze the output by taking into account the corresponding unitary transformation. Since this state analysis only involves orthogonal measurements on individual qubits, the fidelity of the output state is directly given by the fraction of observing the desired state. The measurement results are shown in Fig. 3. All together, 12 single-photon detectors have been used during the whole experiment. The experimental integration time for each possible combination of the input photons was about 50 hours and we recorded about 120 desired two-qubit events. The overall count rate is reduced by a factor of 1/72 due to the success probability of creating the cluster state (1/9), the success probability of the BSMs (1/4) and due to the loss by initializing the input state with polarizers (1/2). On the basis of our original data, we conduct that the average fidelity for the output states of the truth table is 0.72 ± 0.05.

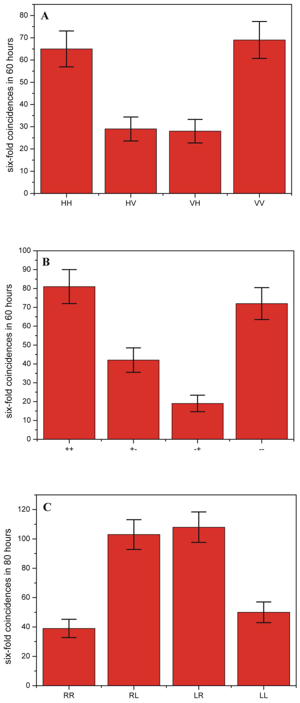

FIG. 4: Experimental results for fidelity measurement of entangled output state. Three complementary basis are used: **(A)** $|H\rangle/|V\rangle$ for the measurement of $\langle\hat{\sigma}_z\hat{\sigma}_z\rangle$; **(B)** $|+\rangle/|-\rangle$ for $\langle\hat{\sigma}_x\hat{\sigma}_x\rangle$ and **(C)** $|L\rangle/|R\rangle = \frac{1}{\sqrt{2}}(|H\rangle \pm i|V\rangle)$ for $\langle\hat{\sigma}_y\hat{\sigma}_y\rangle$. The measured expectation values are: (A) 0.403 ± 0.066 (B) 0.462 ± 0.057 and (C) -0.434 ± 0.062. All errors are of statistical nature and correspond to ± 1 standard deviations.

The determination of the entangling capability is a bit more complex. Since the output state is entangled, we are not able to determine its fidelity by a single measurement setting. However, with three successive local measurements on individual qubits we are still able to accomplish our task. This can be seen by a closer look at the fidelity under scrutiny:

$$\begin{aligned} F &= Tr(\hat{\rho}|\Phi^+\rangle\langle\Phi^+|) \\ &= \frac{1}{4}Tr\left(\hat{\rho}(\hat{I} + \hat{\sigma}_x\hat{\sigma}_x - \hat{\sigma}_y\hat{\sigma}_y + \hat{\sigma}_z\hat{\sigma}_z)\right) \end{aligned} \qquad (4)$$

This implies that by measuring the expectation values $\langle\hat{\sigma}_x\hat{\sigma}_x\rangle$, $\langle\hat{\sigma}_y\hat{\sigma}_y\rangle$, $\langle\hat{\sigma}_z\hat{\sigma}_z\rangle$ we can directly obtain the fidelity of the entangled output state. The experimental results for the correlated local measurement settings are illustrated in Fig. 4. The integration time for the first two settings was about 60 hours and for the third setting about 80 hours. Using the above equation, we determine from our experimental results an fidelity of 0.575 ± 0.027. This is well beyond the state estimation limit of 0.40[27]. Furthermore and most importantly, the result proofs genuine entanglement between the two output photons, since it is above the entanglement limit of 0.50 [28].

All experimental results are calculated directly from the original data and no noise contributions have been subtracted. The imperfection of the fidelities is mainly due to double-pair-emission. Furthermore, the limited interference visibility and imperfect input states also reduce the quality of our output states. Note that we achieve a better fidelity for the truth table than for the entangling case. This is because for the latter one the fidelity depends on the interference visibility at the PBS of the BSM. All given errors are of statistical nature and correspond to ±1 standard deviations.

Some further remarks are warranted here. With our setup we have demonstrated in principle the feasibility of the GC scheme. Note however, that strictly speaking we did not show complete fault-tolerance, since in our experiment we did not encode logic qubits onto a larger number of physical qubits. The principle of the scheme, on the other hand, stays exactly the same and the developed techniques of our setup can be readily extended for the case of a larger number of encoded qubits. Along this line, the generation of a large number of qubits, as well as an improvement of the fidelity – needed for realistic quantum computation – still requires extensive efforts in the future.

In summary, we have experimentally realized a C-NOT gate based on quantum teleportation. With our six-photon architecture we have experimentally demonstrated the ability to entangle two separable qubits and have measured the truth table of the gate. This is the first non-trivial proof-of-principle implementation of the protocol introduced by Gottesman and Chuang. The teleportation-based scheme offers a novel way for scalable quantum computing. Most attractively however, this architecture allows for realizations of universal quantum gates in a fault-tolerant manner, and in fact serves as an important basis for measurement-based quantum computing. Thus, our experimental demonstration represents an important step towards the realization of resource-efficient, scalable quantum computation.

We are thankful for discussions and support on the technological side by Tao Yang and acknowledge insightful discussions with Daniel Gottesman. This work was supported by the Deutsche Forschungsgemeinschaft (DFG), the Alexander von Humboldt Foundation, the European Commission through the ERC Grant and the STREP project HIP the National Fundamental Research Program (Grant No.2006CB921900), the CAS, and the NNSFC. C.W. was additionally supported by the Schlieben-Lange Program of the ESF.

[1] L. K. Grover, Phys. Rev. Lett. **79**, 325 (1997).
[2] P. W. Shor, in *Proceedings of the 35th Annual Symposium on Foundations of Computer Science* (1994).
[3] R. Feynman, International Journal of Theoretical Physics **21**, 467?488 (1982).
[4] J. Preskill, Proc. R. Soc. Lond. A **454**, 385 (1998).
[5] A. M. Steane, Nature **399**, 124 (1999).
[6] D. Gottesman, Phys. Rev. A **57**, 127 (1998).
[7] P. W. Shor, Phys. Rev. A **52**, R2493 (1995).
[8] A. M. Steane, Phys. Rev. Lett. **77**, 793 (1996).
[9] A. R. Calderbank and P. W. Shor, Phys. Rev. A **54**, 1098 (1996).
[10] D. Gottesman, in press (available at http://arxiv.org/abs/quant-ph/9705052).
[11] C. H. Bennett, D. P. DiVincenzo, J. A. Smolin, and W. K. Wootters, Phys. Rev. A **54**, 3824 (1996).
[12] R. Laflamme, C. Miquel, J. P. Paz, and W. H. Zurek, Phys. Rev. Lett. **77**, 198 (1996).
[13] D. Gottesman and I. L. Chuang, Nature **402**, 390 (1999).
[14] R. Raussendorf and H. J. Briegel, Phys. Rev. Lett. **86**, 5188 (2001).
[15] E. Knill, R. Laflamme, and G. J. Milburn, Nature **409**, 46 (2001).
[16] Q. Zhang, A. Goebel, C. Wagenknecht, Y.-A. Chen, B. Zhao, T. Yang, A. Mair, J. Schmiedmayer, and J.-W. Pan, Nature Physics **2**, 678 (2006).
[17] N. Kiesel, C. Schmid, U. Weber, G. Tóth, O. Gühne, R. Ursin, and H. Weinfurter, Phys. Rev. Lett. **95**, 210502 (2005).
[18] A. Barenco, C. Bennett, D. DiVincenzo, N. Margolus, P. Shor, T. Sleator, J. Smolin, and H. Weinfurter, Phys. Rev. A **52**, 3457 (1995).
[19] M. A. Nielsen, Phys. Rev. Lett. **93**, 040503 (2004).
[20] A. M. Goebel, C. Wagenknecht, Q. Zhang, Y.-A. Chen, K. Chen, J. Schmiedmayer, and J.-W. Pan, Phys. Rev. Lett. **101**, 080403 (2008).
[21] C. H. Bennett, G. Brassard, C. Crepeau, R. Jozsa, A. Peres, and W. K. Wootters, Phys. Rev. Lett. **70**, 1895 (1993).
[22] D. Bouwmeester, J.-W. Pan, K. Mattle, M. Eibl, H. Weinfurter, and A. Zeilinger, Nature **390**, 575 (1997).
[23] R. Raussendorf, D. E. Browne, and H. J. Briegel, Phys. Rev. A **68**, 022312 (2003).
[24] P. G. Kwiat, K. Mattle, H. Weinfurter, A. Zeilinger, A. V. Sergienko, and Y. Shih, Phys. Rev. Lett. **75**, 4337 (1995).
[25] C.-Y. Lu, X.-Q. Zhou, O. Gühne, W.-B. Gao, J. Zhang, Z.-S. Yuan, A. Goebel, T. Yang, and J.-W. Pan, Nature Physics **3**, 91 (2007).
[26] J.-W. Pan and A. Zeilinger, Phys. Rev. A **57**, 2208 (1998).
[27] A. Hayashi, T. Hashimoto, and M. Horibe, Phys. Rev. A **72**, 032325 (2005).
[28] O. Gühne, P. Hyllus, D. Bruß, A. Ekert, M. Lewenstein, C. Macchiavello, and A. Sanpera, Phys. Rev. A **66**, 062305 (2002).

APPENDIX. TELEPORTATION-BASED C-NOT GATE

Here, we describe in detail the scheme of a teleportation-based C-NOT gate. We give a step by step analyses of its implementation with our setup, shown in Fig. 2 in the main article.

We align each β-barium borate (BBO) crystal carefully to produce a pair of polarization entangled photons i and j in the state:

$$|\Psi^+\rangle_{ij} = \frac{1}{\sqrt{2}}\left(|H\rangle_i|H\rangle_j + |V\rangle_i|V\rangle_j\right) \tag{5}$$

We use the method described in ref. [17] to prepare the cluster state $|\chi\rangle$. Initially, photons 3, 4, 5 and 6 are in the state:

$$\begin{aligned}|\Psi^+\rangle_{34} &\otimes |\Psi^+\rangle_{56}\\ &= \frac{1}{2}\big(|H\rangle_3|H\rangle_4|H\rangle_5|H\rangle_6 + |H\rangle_3|H\rangle_4|V\rangle_5|V\rangle_6 +\\ &\quad |V\rangle_3|V\rangle_4|H\rangle_5|H\rangle_6 + |V\rangle_3|V\rangle_4|V\rangle_5|V\rangle_6\big).\end{aligned} \tag{6}$$

We direct photons 4 and 6 to the two input modes of a polarization dependent beam splitter (PDBS), respectively. The transmission T_H (T_V) of horizontally (vertically) polarized light at the PDBS is 1 (1/3), and we thus get

$$\begin{aligned}\rightarrow\ &\frac{1}{2}\Big(|H\rangle_3|H\rangle_{4'}|H\rangle_5|H\rangle_{6'} + \frac{1}{\sqrt{3}}|H\rangle_3|H\rangle_{4'}|V\rangle_5|V\rangle_{6'}\\ &+\frac{1}{\sqrt{3}}|V\rangle_3|V\rangle_{4'}|H\rangle_5|H\rangle_{6'}\\ &-\frac{1}{3}|V\rangle_3|V\rangle_{4'}|V\rangle_5|V\rangle_{6'}\Big).\end{aligned} \tag{7}$$

Here we have neglected terms with more than one photon in a single output mode of the PDBS, since in the experiment we post select only terms that lead to a six-fold coincidence.

In order to symmetrize the state we place a PDBS' $(T_H = 1/3, T_V = 1)$ in each output mode of the PDBS and receive

$$\begin{aligned}\rightarrow\ &\frac{1}{6}\big(|H\rangle_3|H\rangle_{4''}|H\rangle_5|H\rangle_{6''} + |H\rangle_3|H\rangle_{4''}|V\rangle_5|V\rangle_{6''}\\ &+|V\rangle_3|V\rangle_{4''}|H\rangle_5|H\rangle_{6''} - |V\rangle_3|V\rangle_{4''}|V\rangle_5|V\rangle_{6''}\big).\end{aligned} \tag{8}$$

This is already the desired four-qubit cluster state up to local unitary operations. To bring it to the desired form, we place half-wave plates (HWPs) – with an angle of 22.5° between the fast and the horizontal axis – into arms 3 and 4. This yields

$$\begin{aligned}\rightarrow\quad &\left(|H\rangle_3|H\rangle_{4''} + |V\rangle_3|V\rangle_{4''}\right)|H\rangle_5|H\rangle_{6''}\\ &+\left(|H\rangle_3|V\rangle_{4''} + |V\rangle_3|H\rangle_{4''}\right)|V\rangle_5|V\rangle_{6''}\\ =\ &|\chi\rangle_{34''56''},\end{aligned} \tag{9}$$

where we have neglected the overall pre-factor 1/6 and we arrive at the desired ancillary four-photon cluster state $|\chi\rangle$ described in ref. [13].

Photons 1 and 2 constitute the input to our C-NOT gate. We assume that they are in a most general input state $|\Psi_{in}\rangle_{12}$, where:

$$\begin{aligned}|\Psi_{in}\rangle_{ij} &= \alpha|H\rangle_i|H\rangle_j + \beta|H\rangle_i|V\rangle_j\\ &\quad+\gamma|V\rangle_i|H\rangle_j + \delta|V\rangle_i|V\rangle_j\end{aligned} \tag{10}$$

The pre-factors α, β, γ and δ are four arbitrary complex numbers satisfying $|\alpha|^2 + |\beta|^2 + |\gamma|^2 + |\delta|^2 = 1$. Before we proceed, let us define the desired output state after a C-NOT operation:

$$\begin{aligned}|\Psi_{out}\rangle_{ij} &= U^{C-NOT}|\Psi_{in}\rangle_{ij}\\ &= \alpha|H\rangle_i|H\rangle_j + \beta|V\rangle_i|V\rangle_j +\\ &\quad \gamma|V\rangle_i|H\rangle_j + \delta|H\rangle_i|V\rangle_j\end{aligned} \tag{11}$$

The target qubit i is flipped on the condition that the control qubit j is in the state $|V\rangle$.

We can now express the combined state of all six photons in terms of Bell states for photons 1&3 and 2&5 and in terms of the desired output state $|\Psi_{out}\rangle_{46}$ for photons 4&6 with corresponding Pauli operations:

$$\begin{aligned}
&|\Psi_{in}\rangle_{12} \otimes |\chi\rangle_{3456} =\\
&\quad |\Phi^+\rangle_{13}|\Phi^+\rangle_{25}\ |\Psi_{out}\rangle_{46} + |\Phi^+\rangle_{13}|\Phi^-\rangle_{25}\ \hat{\sigma}_z^6|\Psi_{out}\rangle_{46}\\
&\quad +|\Phi^+\rangle_{13}|\Psi^+\rangle_{25}\ \hat{\sigma}_x^4\hat{\sigma}_x^6|\Psi_{out}\rangle_{46} + |\Phi^+\rangle_{13}|\Psi^-\rangle_{25}\ \hat{\sigma}_x^4\hat{\sigma}_x^6\hat{\sigma}_z^6|\Psi_{out}\rangle_{46}\\
&\quad +|\Phi^-\rangle_{13}|\Phi^+\rangle_{25}\ \hat{\sigma}_z^4\hat{\sigma}_z^6|\Psi_{out}\rangle_{46} + |\Phi^-\rangle_{13}|\Phi^-\rangle_{25}\ \hat{\sigma}_z^4|\Psi_{out}\rangle_{46}\\
&\quad +|\Phi^-\rangle_{13}|\Psi^+\rangle_{25}\ \hat{\sigma}_x^4\hat{\sigma}_z^4\hat{\sigma}_x^6\hat{\sigma}_z^6|\Psi_{out}\rangle_{46} + |\Phi^-\rangle_{13}|\Psi^-\rangle_{25}\ \hat{\sigma}_x^4\hat{\sigma}_z^4\hat{\sigma}_x^6|\Psi_{out}\rangle_{46}\\
&\quad +|\Psi^+\rangle_{13}|\Phi^+\rangle_{25}\ \hat{\sigma}_x^4|\Psi_{out}\rangle_{46} + |\Psi^+\rangle_{13}|\Phi^-\rangle_{25}\ \hat{\sigma}_x^4\hat{\sigma}_z^6|\Psi_{out}\rangle_{46}\\
&\quad +|\Psi^+\rangle_{13}|\Psi^+\rangle_{25}\ \hat{\sigma}_x^6|\Psi_{out}\rangle_{46} + |\Psi^+\rangle_{13}|\Psi^-\rangle_{25}\ \hat{\sigma}_x^6\hat{\sigma}_z^6|\Psi_{out}\rangle_{46}\\
&\quad +|\Psi^-\rangle_{13}|\Phi^+\rangle_{25}\ \hat{\sigma}_x^4\hat{\sigma}_z^4\hat{\sigma}_z^6|\Psi_{out}\rangle_{46} + |\Psi^-\rangle_{13}|\Phi^-\rangle_{25}\ \hat{\sigma}_x^4\hat{\sigma}_z^4|\Psi_{out}\rangle_{46}\\
&\quad +|\Psi^-\rangle_{13}|\Psi^+\rangle_{25}\ \hat{\sigma}_z^4\hat{\sigma}_x^6\hat{\sigma}_z^6|\Psi_{out}\rangle_{46} + |\Psi^-\rangle_{13}|\Psi^-\rangle_{25}\ \hat{\sigma}_z^4\hat{\sigma}_x^6|\Psi_{out}\rangle_{46}
\end{aligned} \tag{12}$$

With the help of polarizing beam splitters, in our experiment we are able to identify the Bell states $|\Phi^\pm\rangle_{13}$ and

$|\Phi^{\pm}\rangle_{25}$, i.e. we project the combined state of photons 1, 2, 3 and 5 onto one of the four possibilities $|\Phi^{\pm}\rangle_{13}|\Phi^{\pm}\rangle_{25}$. We thus have to consider four different results of the BSMs:

Result of BSMs	Output state
$\|\Phi^{+}\rangle_{13}\|\Phi^{+}\rangle_{25}$	$\|\Psi_{out}\rangle_{46}$
$\|\Phi^{+}\rangle_{13}\|\Phi^{-}\rangle_{25}$	$\hat{\sigma}_z^6\|\Psi_{out}\rangle_{46}$
$\|\Phi^{-}\rangle_{13}\|\Phi^{+}\rangle_{25}$	$\hat{\sigma}_z^4\hat{\sigma}_z^6\|\Psi_{out}\rangle_{46}$
$\|\Phi^{-}\rangle_{13}\|\Phi^{-}\rangle_{25}$	$\hat{\sigma}_z^4\|\Psi_{out}\rangle_{46}$

To receive the desired final state of photons 4 and 6, we have to apply corresponding Pauli operations, depending on the outcome of the BSMs.